J. Biochem. **138**, 563–569 (2005)
doi:10.1093/jb/mvi156

Bacillus circulans MH-K1 Chitosanase: Amino Acid Residues Responsible for Substrate Binding

Tamo Fukamizo[1,*], Satoko Amano[2], Kei Yamaguchi[2], Tomoye Yoshikawa[1], Tomomi Katsumi[1], Jun-ichi Saito[3,†], Michihiko Suzuki[3,†], Kunio Miki[3], Yoshiho Nagata[2] and Akikazu Ando[2]

[1]Department of Advanced Bioscience, Kinki University, 3327-204 Nakamachi, Nara 631-8505; [2]Department of Biotechnology, Graduate School of Science and Technology, Chiba University, Matsudo 271-8510; and [3]Department of Chemistry, Graduate School of Science, Kyoto University, Sakyo-ku, Kyoto 606-8502 Japan

Received May 16, 2005; accepted August 1, 2005

To identify the amino acids responsible for the substrate binding of chitosanase from *Bacillus circulans* MH-K1 (MH-K1 chitosanase), Tyr148 and Lys218 of the chitosanase were mutated to serine and proline, respectively, and the mutated chitosanases were characterized. The enzymatic activities of Y148S and K218P were found to be 12.5% and 0.16% of the wild type, respectively. When the $(GlcN)_3$ binding ability to the chitosanase was evaluated by fluorescence spectroscopy and thermal unfolding experiments, the binding abilities of both mutant enzymes were markedly reduced as compared with the wild type enzyme. The affinity of the enzyme for the trisaccharide decreased by 1.0 kcal/mol of binding free energy for Y148S, and 3.7 kcal/mol for K218P. The crystal structure of K218P revealed that Pro218 forms a *cis*-peptide bond and that the state of the flexible loop containing the 218th residue is considerably affected by the mutation. Thus, we conclude that the flexible loop containing Lys218 plays an important role in substrate binding, and that the role of Tyr148 is less critical, but still important, due to a stacking interaction or hydrogen bond.

Key words: chitosanase, fluorescence, substrate binding, thermal unfolding, X-ray crystallography.

Abbreviations: GlcN, 2-amino-2-deoxy-D-glucopyranose; $(GlcN)_n$, β-1,4–linked oligosaccharide of GlcN with a polymerization degree of *n*; GlcNAc, 2-acetamido-2-deoxy-D-glucopyranose; MH-K1 chitosanase, chitosanase from *Bacillus circulans* MH-K1; N174 chitosanase, chitosanase from *Streptomyces* sp. N174.

Chitosanase from *Bacillus circulans* MH-K1 (MH-K1 chitosanase) is a 29-kDa extracellular protein composed of 259 amino acids (*1*). The enzyme hydrolyzes a β-1,4-glycosidic linkage of chitosan, and belongs to family GH46 according to the classification of Henrissat and Bairoch (*2*). The X-ray crystal structure of MH-K1 chitosanase has already been determined by the multiwavelength anomalous diffraction method (PDB code, 1QGI) (*3*), and is shown in Fig. 1. The enzyme has two globular upper and lower domains, which generate the active site cleft for substrate binding. Chitosanase from *Streptomyces* sp. N174 (N174 chitosanase) belongs to the same glycosyl hydrolase family (*4*); hence, it has a similar fold in its crystal structure (*5*). Thus, the mechanism of the catalytic reaction and substrate recognition of MH-K1 chitosanase might be similar to those of N174 chitosanase. When partially acetylated chitosan was hydrolyzed by individual enzymes, however, a clear difference was found in the cleavage specificity of the two enzymes; that is, MH-K1 chitosanase splits the GlcN-GlcNAc linkage in addition to GlcN-GlcN (*6*), while N174 chitosanase splits the GlcNAc-GlcN linkage in addition to GlcN-GlcN (*7*). Although both enzymes belong to the same hydrolase family and have similar folds, there might be some differences in the mechanism of substrate recognition or binding between these enzymes. In fact, Saito *et al*. have found that the substrate binding cleft of MH-K1 chitosanase is less open than that of N174 chitosanase (*3*). These findings led us to identify the amino acid residues responsible for substrate binding in MH-K1 chitosanase.

It has been recognized that aromatic amino acids are important for protein-carbohydrate interactions (*8*), because the side chains of aromatic amino acids can be involved in various interactions, such as stacking, and hydrophobic and hydrogen bonding interactions, with pyranose rings of the sugar residue (*9–11*). This type of interaction is considered to occur commonly in the complex formation of glycosyl hydrolases with their substrates. However, it is unknown whether the aromatic side chains also play a significant role in the enzyme interaction with polycationic carbohydrates, such as chitosan. An examination of the crystal structure of MH-K1 chitosanase (Fig. 1) revealed that the side chain of Tyr148 is located between two α-helices (α7 and α8) forming the backbone of the substrate binding cleft, and is the sole aromatic residue located at the surface of the substrate binding cleft. The tyrosine residue is conserved in chitosanases belonging to family GH46 and might play an important role in substrate binding. Thus, we substituted Tyr148 with Ser (Y148S) to examine the role of the aromatic side chain.

*To whom correspondence should be addressed. Tel: +81-742-43-8237, Fax: +81-742-43-8976, E-mail: fukamizo@nara.kindai.ac.jp
†Present address: Pharmaceutical Research Institute, Kyowa Hakko Kogyo Co. Ltd., 1188 Shimotogari, Nagaizumi-cho, Sunto-gun, Shizuoka 411-8731.

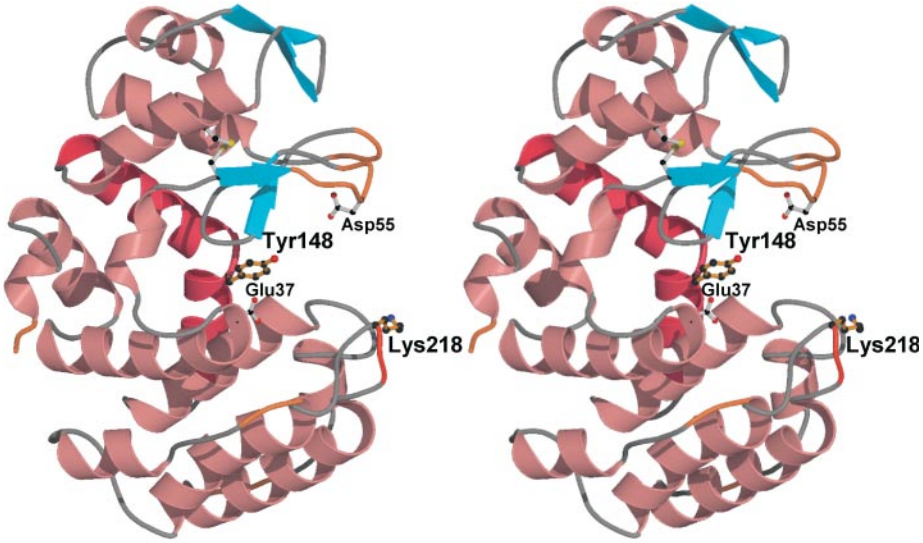

Fig. 1. **Stereoview of the X-ray crystal structure of chitosanase from *Bacillus circulans* MH-K1**. The mutated Tyr148 and Lys218 are highlighted as the ball-and-stick models. Glu37 and Asp55 are the catalytic carboxylates. α-Helices drawn in red are the two important helices forming the backbone of the substrate-binding cleft.

Furthermore, we paid our attention to a flexible loop located at the lower edge of the opened binding cleft (T216–N220, Fig. 1). The temperature factor of the loop region was found to be higher than those of other regions in the crystal structure (*3*). Such a flexible loop at or near the binding cleft has been recognized to play an important role in substrate binding in some glycosyl hydrolases (*12*, *13*). When an *N*-acetylglucosamine residue is docked into the binding cleft, the carbonyl oxygen of the main chain of Lys218 stretches out, resulting in steric hindrance to the *N*-acetyl groups of the sugar. The main chain at the 218th position might participate not only in substrate binding, but also in substrate recognition. Since the loop region is missing in N174 chitosanase, the flexible loop might be the most important structural factor differentiating the cleavage specificity of the two chitosanases. Thus, we substituted Lys218 with Pro (K218P) to fix the main chain conformation of the flexible loop, and to examine the role of the flexible loop in the enzyme function.

The two mutated chitosanases were characterized for their enzyme activity and their substrate binding ability using physicochemical techniques, including thermal unfolding experiments and fluorescence spectroscopy. K218P was further characterized structurally by X-ray crystallography.

MATERIALS AND METHODS

Materials—*Bacillus brevis* strain HPD31-M3 used for the enzyme production was purchased from Higeta Shoyu Co. All reagents for *Bacillus brevis* cultivation and enzyme production were purchased from Wako Pure Chemical Co. CM-TOYOPEARL 650 used for enzyme purification was the product of Tosoh Co. Glucosamine oligosaccharides [$(GlcN)_n$, n = 3–6] were obtained from Seikagaku Kogyo Co. The chitosan substrate used for the preliminary enzyme assay during enzyme purification was purchased from Sigma. All other reagents were commercially available and of analytical grade.

Site-Directed Mutagenesis—Mutations were introduced into the chitosanase (wild type) gene of pKF19k vector using Site-directed Mutagenesis System Mutan^R-Super Express Km (TaKaRa). The PCR primers used for mutagenesis were 5′-TATAACGTGTCTATCCGGTAC-3′ for Y148S and 5′-GATACCAACCCATACAACAAG-3′ for K218P. After confirming the mutation by sequence analysis using an A.L.F DNA Sequencer II (Pharmacia), the resulting mutated genes were excised by *Pst*I and *Eco*RI digestion, subcloned into pNCMO2 vector, and transformed for expression into *B. brevis* by electroporation according to the protocol provided by Higeta Shoyu Co.

Enzyme Production and Purification—The enzymes were produced according to the method of Saito *et al.* (*14*). A colony of *B. brevis* was inoculated into 5 ml of culture medium and cultivated at 30°C for 12 h (subculture). The main culture (100 ml) was cultivated at 30°C for 60 h after the inoculation of 1 ml of the subculture. The culture broth was centrifuged at 10,000 rpm at 4°C for 20 min. Proteins in the supernatant were precipitated by the addition of $(NH_4)_2SO_4$ (to 80% saturation). The precipitate (crude enzyme) was solubilized in a small amount of 20 mM Tris-maleate buffer (pH 6.5 for Y148S, pH5.8 for K218P), and dialyzed against the same buffer overnight. The resultant protein fraction was adsorbed onto a column of CM-TOYOPEARL 650 equilibrated with the same buffer, and eluted with a linear gradient of NaCl (0→0.5 M). The chitosanase fraction was pooled and stored at 4°C for further experiments.

Protein Determination—The protein concentration was determined according to the method of Bradford (*15*) using bovine serum albumin as the standard. For the purified enzyme, the protein concentrations were determined by ultraviolet absorption at 280 nm, using the extinction coefficient calculated from the equation reported by Pace *et al.* (*16*).

SDS-PAGE—SDS–polyacrylamide gel electrophoresis was performed with a 12.5% gel system according to the method of Laemmli (*17*). Protein bands were detected by staining with Coomassie Brilliant Blue R-250.

Enzyme Assay—The chitosanase activity was measured by the method of Fenton *et al.* (*18*). Chitosan 7B (Funakoshi) was used as a substrate. One unit of enzyme activity is the amount of enzyme that releases 1 μmol of reducing sugar, equivalent to glucosamine, per minute.

TLC Determination of the Enzymatic Products—Several microliters of the enzyme solution dialyzed against 50 mM sodium acetate buffer, pH 5.0, were added to 0.5 ml of $(GlcN)_6$ solution dissolved in the same buffer. The enzymatic reaction was conducted at 40°C, and an aliquot withdrawn from the reaction mixture at each reaction time was spotted onto a TLC aluminium sheet (20 × 20 cm, Silica gel 60, MERCK). The TLC sheet was developed in a solvent system composed of *n*-propylalcohol and 28% ammonium hydroxide (2:1). After drying the sheet, the glucosamine residues were detected by spraying with ninhydrin reagent.

Fluorescence Spectroscopy—Fluorescence spectra were recorded at an excitation wavelength of 295 nm using a Hitachi F-3010 spectrofluorometer. The enzyme preption was dialyzed against 0.06 M Tris-HCl buffer, pH 7.0, containing 0.1 M NaCl before the measurement. Various concentrations of glucosamine trisaccharide [$(GlcN)_3$] dissolved in the same buffer were added to the enzyme solution, and the spectra of the enzyme-saccharide mixtures were obtained. The relative changes in the fluorescence intensity, $1 - (F_1/F_0)$, were plotted against substrate concentration, and the dissociation constants were determined by a nonlinear least square fitting procedure based on the Scatchard equation,

$$\Delta F = \Delta F_{max} \cdot [S]/(K_d + [S]),$$

where ΔF and ΔF_{max} indicate the relative fluorescence change and its maximum, respectively. K_d is the dissociation constant, and [S] is the free saccharide concentration. Under our experimental conditions, the concentrations of the $(GlcN)_3$ solutions added were in 1,000-fold excess to the enzyme concentration. Thus, the value of [S] can be regarded as being almost equal to the added $(GlcN)_3$ concentration. When *N*-acetyltryptophan ethylester was used instead of the enzyme, no appreciable change was found in the fluorescence intensity. This indicates that the fluorescence change observed for the enzyme–trisaccharide mixture is derived from the trisaccharide binding to the enzyme.

Circular Dichroism—CD spectra of the chitosanases were obtained in 50 mM sodium phosphate buffer, pH 7.0, using a Jasco J-720 spectropolarimeter (cell length, 0.1 cm) at 20°C.

Thermal Unfolding Experiments—To obtain thermal unfolding curves of chitosanases in the presence or absence of $(GlcN)_3$, the CD value at 222 nm was monitored while the temperature was raised at a rate of 1°C per min. The trisaccharide solution was added to the enzyme solution to examine the effect of binding on the thermal stability. Concentrations of the enzyme and $(GlcN)_3$ were 2.5 μM and 2.5 mM, respectively. The temperature was measured using a DP-500 thermometer (Rikagaku kogyo). The experimental data were normalized by linearly extrapolating the pre- and post-transition baselines into the transition zone, and then plotted against temperature. Under the assumption that the unfolding transition of the chitosanase follows a two-state mechanism, the unfolding curves were subjected to least squares analysis in order to obtain the transition temperatures of thermal unfolding (T_m). Thermodynamic parameters could not be obtained because of the poor reversibilities of protein unfolding.

X-Ray Crystallography—The purified K218P mutant chitosanase was concentrated using Centriprep^R (MILLIPORE) to 31 mg/ml for crystallization. Crystallization of K218P was performed at 20°C by the sitting drop vapor diffusion method using ammonium sulfate as the precipitant. Intensity data on the K218P chitosanase crystal were collected in a home laboratory using a Rigaku R-Axis IV^{++} imaging plate detector on a Rigaku rotating anode UltraX18 X-ray generator, with a mirror-focused optics CuKα X-ray operating at 50 kV and 100 mA. The intensity data were processed and merged using the programs *DENZO* (*19*) and *SCALEPACK*. The structure was solved by molecular replacement (MR) using the program *AMoRe* in the *CCP4* suite (*20*, *21*). A high-resolution and well-refined wild type MH-K1 chitosanase (PDB code 1QGI) (*3*) was used as the search model for MR. Structural refinements were made using the *X-PLOR* program (*22*). This refined model was subjected to molecular dynamics and simulated annealing refinement with slow cooling from 3,000 to 300 K at 5.0–2.0 Å resolution. After repeated manual rebuilding and fitting the model into $2F_o - F_c$ and $F_o - F_c$ maps using the program *TURBO-FRODO* (*23*), positional and individual atomic B factor refinements were carried out. The stereochemistry of the final model was analyzed using the program *PROCHECK* (*24*).

Protein Data Bank Entry—The atomic coordinates of the K218P mutant chitosanase have been deposited in the Protein Data Bank as entry 2D05.

RESULTS

Production and Purification of the Mutant Chitosanases—The wild type, Y148S, and K218P MH-K1 chitosanases were successfully produced by the *B. brevis* expression system. The amounts of mutant proteins produced from 500 ml of culture supernatant were 113 mg for Y148S and 131 mg for K218P, while 148 mg of the wild type protein was obtained from the same volume of culture supernatant. The efficiency of protein secretion was not greatly suppressed by the mutations. Each mutated enzyme was successfully purified from the culture supernatant by CM-TOYOPEARL column chromatography, and appeared as a single band on SDS-PAGE (data not shown). The CD spectra of the wild type and mutant chitosanases exhibited similar profiles (data not shown), indicating that the global conformation is not affected by the mutation.

Enzymatic Activities of the Mutant Chitosanases—At first, the purified mutant chitosanases were subjected to activity determination using the substrate Chitosan 7B (20% acetylated chitosan). When the reducing sugars produced from the substrate (0.8 mg/ml) were determined for the individual enzymes, the activities of Y148S and K218P were found to be 12.5% and 0.16% of the wild type enzyme, respectively. Activity measurements were also conducted with TLC analysis using the substrate, $(GlcN)_6$. Figure 2 shows the TLC profiles of the products obtained from the chitosanase-catalyzed hydrolysis of the hexasaccharide. The wild type enzyme produced $(GlcN)_2$, $(GlcN)_3$ and $(GlcN)_4$ in almost equivalent amounts. This suggests that the enzyme hydrolyzes $(GlcN)_6$ in an endo-splitting manner. When the Y148S mutant was used instead of the wild type, the rate of degradation of $(GlcN)_6$ was much lower than that of the wild type enzyme reaction.

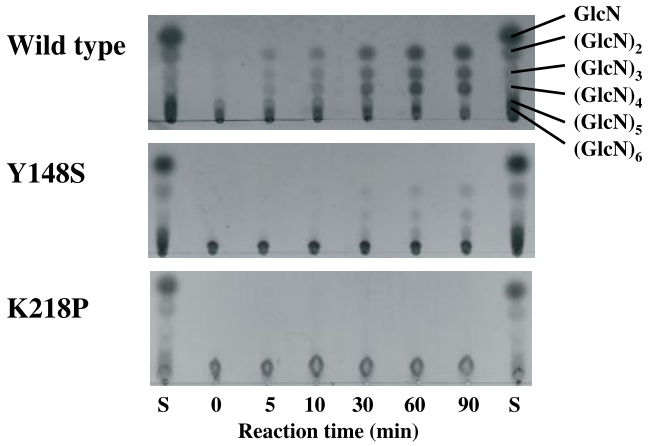

Fig. 2. **TLC profiles showing the $(GlcN)_6$ hydrolysis catalyzed by chitosanases.** The enzymatic reaction was conducted in 50 mM sodium acetate buffer at pH 5.0 at 40°C. The enzyme and substrate concentrations were 0.2 μM and 15 mM, respectively.

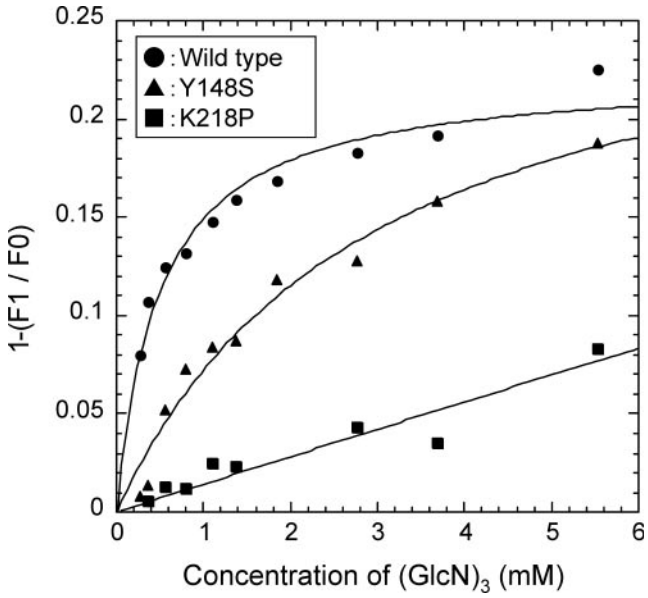

Fig. 3. **$(GlcN)_3$ binding to chitosanase as determined by fluorescence spectroscopy.** F_1/F_0 indicates the relative fluorescence intensity with $(GlcN)_3$ to that without the trisaccharide. The enzyme concentration was 2.5 μM. The fluorescence measurements were conducted in 0.06 M Tris-HCl buffer at pH 7.0 containing 0.1 M NaCl.

When the product distribution at 5 min of the wild type reaction is compared with that at 90 min of the Y148S reaction, no appreciable difference was found. This suggests that the Tyr148 mutation affects substrate affinity without changing the binding mode. For the K218P mutant, any products were hardly detected, indicating that the enzymatic activity was eliminated by the mutation. The values of the steady state kinetic pmeters, K_m and k_{cat}, could not be determined accurately because of the substrate inhibition.

Fluorescence Analysis of Substrate Binding—When $(GlcN)_3$ was added to the chitosanase solution, the fluorescence intensity clearly decreased in a concentration-dependent manner (data not shown). The relative decreases in the fluorescence intensity were plotted against the substrate concentration to obtain saturation curves (Fig. 3). Based on the saturation curves, the binding constants of $(GlcN)_3$ to the wild type, Y148S, and K218P chitosanases were calculated to be 2,009 ± 15, 341 ± 01, and 3.4 ± 02 M^{-1}, respectively. These values correspond to binding free energy changes of –6.8, –5.8, and –3.1 kcal/mol. The binding abilities of both mutant enzymes were markedly reduced as compared with the wild type enzyme. The free energy changes in saccharide binding decreased by 1.0 kcal/mol for Y148S and by 3.7 kcal/mol for K218P. These values are summarized in Table 1. GlcN and $(GlcN)_2$ did not significantly affect the fluorescence intensity because of their lower binding abilities. $(GlcN)_n$ ($n \geqslant 4$) were not tested, because the oligosaccharides are immediately degraded by the enzyme.

Thermal Unfolding Experiments—The transition temperature of thermal unfolding (T_m) of the wild type protein was determined to be 53.9°C. When one thousand molar excess of $(GlcN)_3$ was added to the wild type enzyme, the T_m value was 56.1°C ($\Delta T_m = 2.2$°C) as shown in Fig. 4A. The increase in T_m is due to the binding interaction between the enzyme and the trisaccharide (*25*). When Y148S was used instead of the wild type, the T_m value was 53.1°C, and increased by 0.7°C upon the addition of $(GlcN)_3$. The ΔT_m value was significantly suppressed as compared with the wild type (Fig. 4B). For K218P, the T_m value was 55.1°C in the absence of $(GlcN)_3$ (Fig. 4C). The mutation of Lys218 to Pro might suppress the flexibility of the loop, resulting in a stabilization of the overall protein structure. The addition of $(GlcN)_3$ did not cause any increase in T_m, but rather decreased the transition temperature by 1.2°C (Fig. 4C). The decrease in T_m cannot be explained at present, but at least suggests that $(GlcN)_3$ does not interact correctly with K218P. The mutated enzyme might fail to accept the trisaccharide molecule correctly because of the lower flexibility of the loop structure. Such incorrect binding of $(GlcN)_3$ might destabilize the structure of K218P. The T_m values obtained are listed in Table 2.

Table 1. **Binding constants of $(GlcN)_3$ to the wild type and mutant chitosanases from *Bacillus circulans* MH-K1.**

Chitosanase	Binding constant (M^{-1})	Binding free energy (kcal/mol)
Wild type	2,009 ± 15	–6.8
Y148S	341 ± 01	–5.8
K218P	3.4 ± 02	–3.1

X-Ray Crystal Structure of the Mutant Chitosanase—To identify the structural factors bringing about the lower binding ability, we attempted to solve the crystal structure of K218P. Crystals of the K218P mutant chitosanase were found to belong to the orthorhombic space group $P2_12_12$ with unit-cell dimensions of a = 43.3 Å, b = 128.1 Å and c = 57.8 Å, almost the same as the wild type crystal. The crystal structure of the K218P mutant chitosanase was solved using molecular replacement as described in "MATERIALS AND METHODS." the crystallographic r factor for the final model, including 200 water molecules and an SO_4^{2-} ion lying on the crystallographic 2-fold axis, was 17.3% (R_{free} 21.3%) at 2.0 Å resolution (Table 3).

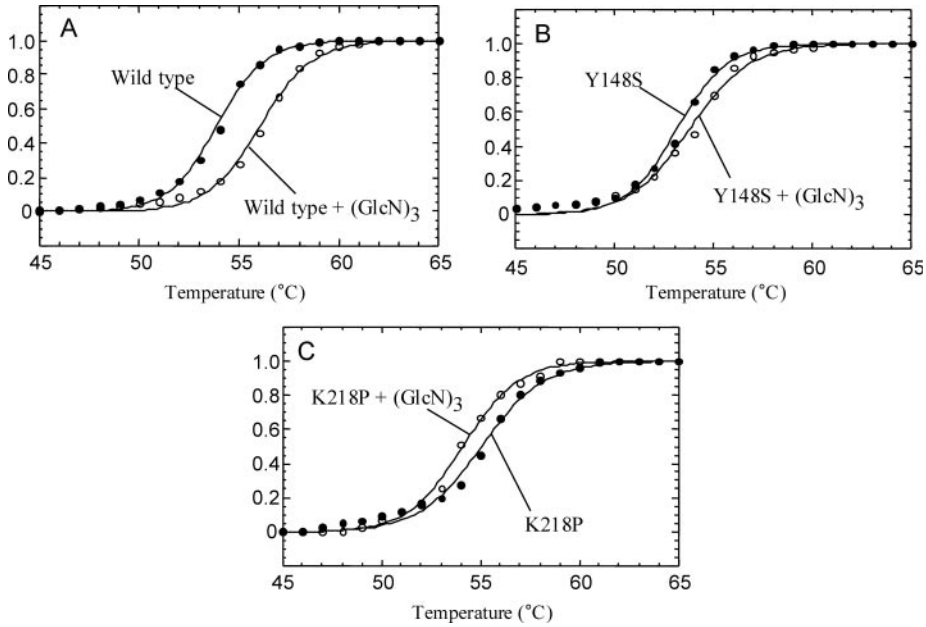

Fig. 4. **Thermal unfolding curves of the wild type (A) and mutated MH-K1 chitosanases, Y148S (B) and K218P (C)**. The unfolding transition was conducted in 50 mM sodium phosphate buffer, pH 7.0, at 20°C. The concentration of each enzyme was 2.5 μM. A 1,000-fold molar excess of $(GlcN)_3$ was added to each enzyme solution to examine the binding effect.

Table 2. **The transition temperature of thermal unfolding, T_m, and the T_m elevation upon the addition of $(GlcN)_3$, ΔT_m, for wild type, Y148S, and K218P chitosanases.**

	T_m (°C)	ΔT_m (°C)
Wild type	53.9	
+$(GlcN)_3$	56.1	2.2
Y148S	53.1	
+$(GlcN)_3$	53.8	0.7
K218P	55.1	
+$(GlcN)_3$	53.9	–1.2

Table 3. **Statistics of data collection and structure determination for the K218P mutant chitosanase.**

Data collection	
Unit cell (Å)	a = 43.3
	b = 128.1
	c = 57.8
Space group	$P2_12_12$
Resolution (Å)	100–2.0 (2.07–2.00)
Total observed reflections	122,760
Unique reflections	22,593
Completeness (%)	88.5 (79.1)
R_{merge} (%)	11.0 (48.7)
I/sig$I$	15.8 (4.6)
Structure refinement	
No. of water molecules	200
No. of ions (SO_4^{2-})	1 on 2-fold axis
R-factor[a] (%)	17.3
R-free[b] (%)	21.3
RMS deviations	
bonds (Å)	0.010
angles (deg.)	1.452

[a]R factor = $\Sigma \mid F_{obs} - F_{calc} \mid / \Sigma \mid F_{obs} \mid$, where F_{obs} and F_{calc} are the observed and calculated structure factor amplitudes, [b]The R_{free} value was calculated from a set of reflections (5%) randomly, which were omitted from structure refinement.

A superposition of the overall structures of the mutant and wild type chitosanases (*3*) is shown in Fig. 5A. The root mean square deviation for all corresponding Cα atoms was 0.51 Å. As estimated from the CD spectra, the global conformation was not greatly affected by the mutation. A closer examination of the structures, however, revealed that the flexible loop containing the mutated 218th residue was remarkably shifted, and that the orientation of the Asn217 side chain was rearranged due to the mutation. These structural changes appear to result from a *cis*-peptide bond formation at Pro218 (Fig. 5B). The side chain of Lys218 in the wild type chitosanase is supposed to form a hydrogen bonding network via several water molecules, which might contribute to the stability of the active site architecture and influence the protonation state of the two catalytic residues. The hydrogen bonding network might be disrupted in the K218P mutant. This situation would affect the binding and catalytic activities of the enzyme, resulting in the heavy loss of enzymatic activity.

DISCUSSION

The substrate-binding cleft of *Streptomyces* sp. N174 chitosanase has been reported to be composed of six subsites (–3) to (+3) (*26*). Negative charges are predominant in the entire region of the binding cleft. Thus, electrostatic interaction has been regarded as one of the most probable mechanisms for substrate binding to chitosanase because of the polycationic properties of the substrate polysaccharide. In fact, an aspartic acid residue (Asp57) has been identified to be an important residue for substrate binding in N174 chitosanase (*26*). A similar substrate-binding cleft, (–3) to (+3), and a similar binding mode would occur in MH-K1 chitosanase because the three dimensional structure is closely related to that of N174 chitosanase. However, it is reasonable to pay attention to the aromatic side chains because stacking interactions

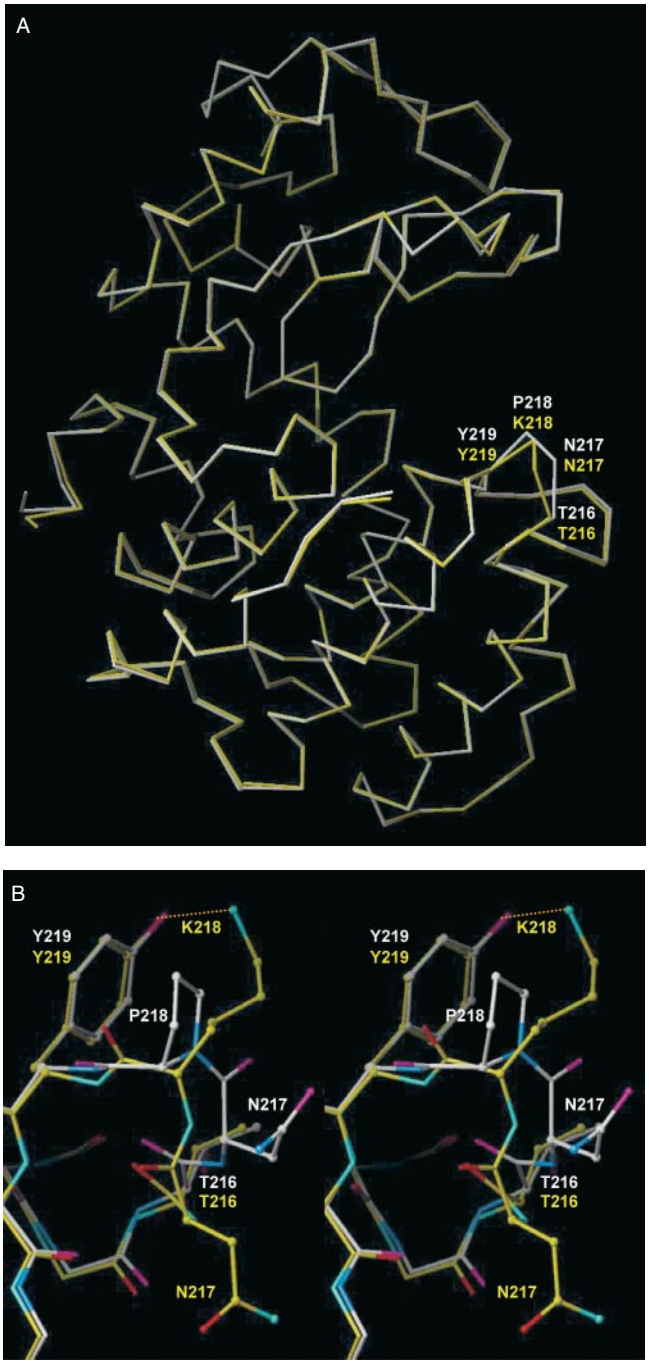

Fig. 5. **Superposition of the crystal structures of the wild type and K218P MH-K1 chitosanases**. (A) Cα traces of the wild type (yellow) and K218P (white). (B) Stereo view of a close-up of the mutation position (Lys218). Labels are amino acid residues of the wild type (yellow) and K218P (white). Dotted lines indicate a hydrogen bond between the side chains of Lys218 and Tyr219 of the wild type enzyme.

with the substrate pyranose rings have been recognized to participate in protein-carbohydrate interactions (*8*). In this study, the substitution of Tyr148 with Ser was found to reduce the binding affinity for $(GlcN)_3$ by about 1.0 kcal/mol of binding free energy. The lower binding ability of Y148S was confirmed by the thermal unfolding experiments (Fig. 3B). The free energy difference, 1.0 kcal/mol, can be regarded as the free energy contribution of the stacking interaction through the aromatic ring as well as hydrogen bonding through the hydroxyl group of Tyr148. The low enzymatic activity of Y148S (12.5% of the wild type enzyme) should derive at least in part from the suppression of binding ability. It is reasonable to assume that the mutation of Tyr148 might not only affect the binding ability at the corresponding subsite, but impair the catalytic efficiency by affecting the conformational state of the catalytic cleft. In fact, in N174 chitosanase, the mutation of Asp57, which participates in sugar residue binding at the (–2) site, affects not only the binding affinity at the subsite, but also the rate constant for the cleavage of β-1,4-glycosidic linkages (*26*). A similar effect might occur in the Tyr148 mutation of MH-K1 chitosanase.

A positively charged lysine residue in a moderate pH region cannot generally be regarded as a candidate for the amino acid residue responsible for substrate recognition or binding in chitosanases because of electrostatic repulsion with the polycation of the chitosan substrate. In this study, however, the mutation of Lys218 to Pro strictly eliminated the enzymatic activity. The binding constant of $(GlcN)_3$ was severely depressed in K218P by about 3.7 kcal/mol of binding free energy. The flexible loop comprising Lys218 is likely very important for substrate binding. To rationalize the importance of the flexible loop, the three dimensional structure of K218P was solved by X-ray crystallography. We found from the crystal structure that Pro218 has a *cis*-peptide bond, and that the main chain and side chain structures of the loop containing the 218th residue are considerably affected by the mutation. A few neighboring amino acids are considered to have a direct influence on the probability of forming a *cis* prolyl residue (*27*). Aromatic amino acids preceding or succeeding the respective proline residue appear to increase the probability of *cis* prolyl peptide formation. In MH-K1 chitosanase, Tyr219 might positively influence *cis* prolyl peptide formation. In the crystal structure of the wild type chitosanase, the loop containing Lys218 is located at the lower edge of the binding cleft, and the temperature factor of this loop region was found to be relatively high (*3*). It has been recognized that such a flexible loop plays an important role in substrate binding in some carbohydrate-active enzymes. The flexible loop of human salivary amylase is considered to assist catalysis during the transition state, and to play a role in releasing the product from the active site (*12*). When an oligosaccharide inhibitor binds to *Bacillus cereus* amylase, the flexible loop (residues 93–97) was found to move dramatically and cover the bound inhibitor (*13*). Similarly, the flexible loop containing Lys218 in MH-K1 chitosanase performs a very important action toward the substrate in positioning it correctly in the enzyme. The mutation of Lys218 to proline greatly alters the conformation and flexibility of the loop structure. In addition, Lys218 in the wild type MH-K1 chitosanase is supposed to participate in a hydrogen bonding network with neighboring amino acids through the aid of several water molecules. The lysine mutation to proline might disrupt these hydrogen bonds, resulting in a considerable change in the conformation of the catalytic cleft. It is likely that the Lys218 mutation affects the catalytic efficiency of the proton donor carboxylate (Glu37). Nevertheless, main chain flexibility might be

suppressed by the *cis* conformation of the prolyl peptide at the 218th position. Such a complicated situation surrounding the loop containing Pro218 would interfere with its correct action toward the substrate, ultimately resulting in the heavy loss of the enzymatic activity.

In conclusion, the low enzymatic activities of the mutant enzymes, Y148S and K218P, are due at least in part to a decrease in substrate binding ability. The crystal structure of K218P revealed that the main chain and side chain conformations of the loop comprising the 218th residue are considerably affected by the mutation. The flexible loop containing Lys218 plays an important role in substrate binding, and the role of Tyr148 is less critical, but still important, probably due to a stacking interaction or a hydrogen bond.

REFERENCES

1. Ando, A., Noguchi, K., Yanagi, M., Shinomiya, H., Kagawa, W., Hirata, H., Yabuki, M., and Fujii, T. (1992) Primary structure of chitosanase produced by *Bacillus circulans* MH-K1. *J. Gen. Appl. Microbiol.* **38**, 135–144
2. Henrissat, B. and Bairoch, A. (1996) Updating the sequence-based classification of glycosyl hydrolases. *Biochem. J.* **316**, 695–696
3. Saito, J., Kita, A., Higuchi, Y., Nagata, Y., Ando, A., and Miki, K. (1999) Crystal structure of chitosanase from *Bacillus circulans* MH-K1 at 1.6-Å resolution and its substrate recognition mechanism. *J. Biol. Chem.* **274**, 30818–30825
4. Fukamizo, T. and Brzezinski, R. (1997) Chitosanase from *Streptomyces* sp. strain N174: a comptive review of its structure and function. *Biochem. Cell Biol.* **75**, 687–696
5. Marcotte, E.M., Monzingo, A.F., Ernst, S.R., Brzezinski, R., and Robertus, J.D. (1996) X-ray structure of an antifungal chitosanase from *Streptomyces* N174. *Nature Struct. Biol.* **3**, 155–162
6. Mitsutomi, M., Ueda, M., Arai, M., Ando, A., and Watanabe, T. (1996) Action patterns of microbial chitinases and chitosanases on partially *N*-acetylated chitosan. In *Chitin Enzymology*, Vol. 2, pp. 273–284
7. Fukamizo, T., Honda, Y., Goto, S., Boucher, I., and Brzezinski, R. (1995) Reaction mechanism of chitosanase from *Streptomyces* sp. N174. *Biochem. J.* **311**, 377–383
8. Vyas, N.K. (1991) Atomic features of protein-carbohydrate interactions. *Curr. Opin. Struct. Biol.* **1**, 732–740
9. Maenaka, K., Kawai, G., Watanabe, K., Sunada, F., and Kumagai, I. (1994) Functional and structural role of a tryptophan generally observed in protein-carbohydrate interaction. *J. Biol. Chem.* **269**, 7070–7075
10. Watanabe, T., Ariga, Y., Sato, U., Toratani, T., Hashimoto, M., Nikaidou, N., Kezuka, Y., Nonaka, T., and Sugiyama, J. (2003) Aromatic residues within the substrate-binding cleft of *Bacillus circulans* chitinase A1 are essential for hydrolysis of crystalline chitin. *Biochem. J.* **376**, 237–244
11. Katouno, F., Taguchi, M., Sakurai, K., Uchiyama, T., Nikaidou, N., Nonaka, T., Sugiyama, J., and Watanabe, T. (2004) Importance of exposed aromatic residues in chitinase B from *Serratia marcescens* 2170 for crystalline chitin hydrolysis. *J. Biochem.* **136**, 163–168
12. Ramasubbu, N., Ragunath, C., and Mishra, P.J. (2003) Probing the role of a mobile loop in substrate binding and enzyme activity of human salivary amylase. *J. Mol. Biol.* **325**, 1061–1076
13. Oyama, T., Miyake, H., Kusunoki, M., and Nitta, Y. (2003) Crystal structures of beta-amylase from *Bacillus cereus* var. *mycoides* in complexes with substrate analogs and affinity-labeling reagents. *J. Biochem.* **133**, 467–474
14. Saito, J., Kita, A., Nagata, Y., Ando, A., and Miki, K. (1995) Crystallization and preliminary X-ray crystallographic analysis of chitosanase from *Bacillus circulans* MH-K1. *Acta Crystallogr. Sec. D* **51**, 856–857
15. Bradford. M.M. (1976) A rapid and sensitive method for the quantitation of microgram quantities of protein utilizing the principle of protein-dye binding. *Anal. Biochem.* **72**, 248–254
16. Pace, C.N., Vajdos, F., Fee, L., Grimsley, G., and Gray, T. (1995) How to measure and predict the molar absorption coefficient of a protein. *Protein Sci.* **4**, 2411–2423
17. Laemmli, U.K. (1970) Cleavage of structural proteins during the assembly of the head of bacteriophage T4. *Nature* **227**, 680–685
18. Fenton, D.M. and Eveleigh, D.E. (1981) Purification and Mode of Action of a Chitosanase from *Penicillium islandicum*. *J. Gen. Microbiol.* **126**, 151–165
19. Otwinowski, Z. and Minor, M. (1997) Processing of X-ray diffraction data collected in oscillation mode. *Methods Enzymol.* **276**, 307–326
20. Navaza, J. (2001) Implementation of molecular replacement in *AMoRe*. *Acta Crystallogr. Sec. D* **57**, 1362–1372
21. Collaborative Computational Project 4 (1994) The *CCP*4 suite: programs for protein crystallography. *Acta Crystallogr. Sec. D* **50**, 760–763
22. Brünger, A.T. (1993) *XPLOR Version 3.1 Manual*, Yale University
23. Roussel, A. and Cambillau, C. (1992) *TURBO-FRODO*, Biographics, LCCMB, Marseille, France
24. Laskowski, P.V., MacArthur, M.W., Moss, D.S., and Thornton, J.M. (1994) *PROCHECK*: a program to check the stereochemical quality of protein structures. *J. Appl. Crystallogr.* **26**, 283–291
25. Honda, Y. and Fukamizo, T., Boucher, I., and Brzezinski, R. (1997) Substrate binding to the inactive mutants of *Streptomyces* sp. N174 chitosanase: indirect evaluation from the thermal unfolding experiments. *FEBS Lett.* **411**, 346–350
26. Tremblay, H., Yamaguchi, T., Fukamizo, T., and Brzezinski, R. (2001) Mechanism of chitosanase-oligosaccharide interaction: Subsite structure of Streptomyces sp. N174 chitosanase and the role of Asp57 carboxylate. *J. Biochem.* **130**, 679–686
27. Lorenzen, S., Peters, B., Goede, A., Preissner, R., and Frömmel, C. (2005) Conservation of *cis* prolyl bonds in proteins during evolution. *Proteins: Structure, Function, and Bioinformatics* **58**, 589–595